Dynamics of Electron Localization in Warm versus Cold Water Clusters

Ondrej Marsalek,[1] Frank Uhlig,[2] Tomaso Frigato,[3] Burkhard Schmidt,[3] and Pavel Jungwirth[1,*]

[1]*Institute of Organic Chemistry and Biochemistry, Academy of Sciences of the Czech Republic and Center for Biomolecules and Complex Molecular Systems, Flemingovo nám. 2, CZ-16610 Prague 6, Czech Republic*

[2]*Wilhelm-Ostwald-Institut für Physikalische und Theoretische Chemie, Linnéstraße 2, D-04103 Leipzig, Germany*

[3]*Institut für Mathematik, Freie Universität Berlin, Arnimallee 6, D-14195 Berlin, Germany*

(Received 5 March 2010; published 21 July 2010)

The process of electron localization on a cluster of 32 water molecules at 20, 50, and 300 K is unraveled using *ab initio* molecular dynamics simulations. In warm, liquid clusters, the excess electron relaxes from an initial diffuse and weakly bound structure to an equilibrated, strongly bound species within 1.5 ps. In contrast, in cold, glassy clusters the relaxation processes is not completed and the electron becomes trapped in a metastable surface state with an intermediate binding energy. These results question the validity of extrapolations of the properties of solvated electrons from cold clusters of increasing size to the liquid bulk.

DOI: 10.1103/PhysRevLett.105.043002 PACS numbers: 31.15.es, 33.15.Ry, 33.80.Eh

Interaction of ionizing radiation with water leads to formation of a quasifree electron and a partially delocalized cationic hole. Both of these species undergo ultrafast reactive dynamics. H_2O^+ reacts on a 100 fs time scale with a neighboring water molecule forming H_3O^+ and OH [1,2]. The latter is a key radical involved in indirect radiation damage of DNA. In this process, the quasifree electron also plays a role [1,3]; however, the aqueous environment causes its localization and formation of a solvated electron on a picosecond time scale [4,5]. Depending on water purity, solvated electrons survive for up to microseconds or milliseconds before reacting with salt ions, dissolved oxygen molecules, OH radicals, protons, or water molecules themselves [1,6–10]. These are fundamental reactions in radiation chemistry, which are important, among others, in nuclear waste treatment [1].

A very detailed molecular insight into the structure of an electron in aqueous environment has been gained from cluster studies. Both experiments and calculations show that the character of this species changes from a weakly (dipole) bound electron in small water clusters to a more bulklike solvated electron in larger clusters [11–19]. This behavior has been utilized for extrapolating the binding energy and other properties of the electron from clusters of increasing size into the aqueous bulk [12,20]. These extrapolations are, however, not free of contradictions, which concern the occurrence of several isomers and electron binding motifs, as well as surface vs interior location of the electron in water clusters of different sizes [12,14,19]. A crucial issue, which has gained more attention recently [15,21] and will be addressed in this study, is the fact that extrapolations to liquid water are done using clusters at very low (typically below 100 K) temperatures. Under these conditions, clusters with tens to hundreds of water molecules are unlikely to be liquid, but rather resemble amorphous solids [22]. In such a glassy state, translational motion is dramatically slowed down. Therefore, kinetically trapped electron-cluster geometries which depend on preparation conditions, rather than fully relaxed structures, can prevail in the experiment [12,15]. Measurements and simulations show that the observed state sensitively depends on the history of the cluster both before and after electron attachment [15,21].

Here, we address the question of electron localization on medium-size water clusters at warm vs cold conditions using *ab initio* molecular dynamics (AIMD) simulations. Initially, an electron is vertically (i.e., without any geometry change) attached to a neutral cluster comprising 32 water molecules and its subsequent dynamics is followed at cluster temperatures ranging from 20 to 300 K. We show below that the resulting localization process dramatically depends on temperature, which puts a question mark over extrapolations from cold clusters to the liquid bulk.

The computational methodology has been described in detail in our recent paper on electron-proton recombination in water [9]. Briefly, we perform AIMD using the BLYP density functional [23,24] with a dispersion correction [25]. Pseudopotentials [26] replace the oxygen core electrons and the hybrid Gaussian plane wave scheme is used for efficient evaluation of the energies and forces [27]. The self-interaction correction is employed for the singly-occupied orbital in a restricted open-shell Kohn-Sham framework [28]. The Kohn-Sham orbitals are represented using a TZV2P basis set [29] augmented with diffuse Gaussian functions placed on a regular grid spanning the whole simulation box. Open boundary conditions together with a suitable electrostatic solver [30] are used, as is appropriate for a cluster system. The vertical detachment energy (VDE) is calculated directly from the energy difference between the anionic and the neutral system at the same geometry. The excess electron is plotted as the unpaired spin density of the system [31]. Comparison to RIMP2 calculations suggests that the present DFT calculations only slightly overestimate the VDE of the excess

electron [31]. The present way of correcting the self-interaction error improves the description of the anionic cluster at the expense of artificially increasing the VDE. Compared to previously used one-electron models [19,32] the all (valence) electron AIMD approach adopted here explicitly accounts for coupling between the excess electron and valence electrons of water molecules [33].

All the localization trajectories were started from the geometry of a neutral water cluster. For comparison, equilibrium trajectories were also performed, started with a preexisting polarized cavity [31]. Initial geometries for localization at low temperatures were obtained by energy minimization, while the 300 K simulations used snapshots from dynamics at 300 K as their initial condition. All production simulations were performed at constant total energy using the CP2K package [34].

We simulated six localization trajectories with an electron added to a cluster of 32 water molecules equilibrated at 300 K. Figure 1 shows three snapshots from a representative trajectory, taken at 0, 950, and 4250 fs. Upon attachment to the neutral cluster, the excess electron is initially delocalized over the outer surface of the water cluster [Fig. 1(a)], with a radius of gyration of about 6 Å. However, the excess electron immediately starts to shrink, polarizing neighboring water molecules. This localization process can be roughly separated into two steps. First, water molecules locally reorient forming the initial solvation structure within less than a picosecond [Fig. 1(b)]. The structure then becomes even more favorable for electron binding by translational and further rotational motion of water molecules. This process creates a polarized cavity and moves the electron deeper into the cluster. Nevertheless, for most of the simulation time the electron remains solvated asymmetrically with respect to the center of the cluster, i.e., close to the surface [Fig. 1(c)]. In less than 1.5 ps the electron thus acquires its final size of about 2.75 Å and becomes indistinguishable from an equilibrated solvated electron in a 32 water cluster, as investigated in our previous study [31].

The main physical characteristics, i.e., radius of gyration, VDE, and average distance from the cluster center of mass (COM) [31] of the excess electron along the trajectory depicted in Fig. 1 are plotted in Fig. 2. The top panel shows the process of shrinking of the excess electron from its initial size of 6 Å to about 5 Å in less than 1 ps, and then to the final value of ~2.75 Å in another 0.5 ps. The middle panel depicts the VDE, the negative value of which strongly correlates with the radius of gyration of the excess electron, as observed also for the equilibrated solvated electron [31]. The initial delocalized electron is bound to the neutral water cluster by less than 1 eV; however, within 1.5 ps its vertical binding energy triples, fluctuating around its final value of about 3 eV. The last panel of Fig. 2 shows the time evolution of the average distance of the excess electron from the COM of the water cluster [31]. This distance decreases from its initial value of 6 Å to about 5 Å. The excess electron is thus brought closer to the COM of the cluster by the localization process. Nevertheless, it remains to be situated predominantly in the interfacial region, in agreement with previous studies of an equilibrium solvated electron in a cluster of the same size [19,31]. Finally, note that there is little correlation between the position of the excess electron within the cluster and its vertical binding energy [31].

Time evolution of the radius of gyration of the excess electron [9] for the six simulated trajectories at 300 K is depicted in Fig. 3. Because of different geometries of the neutral clusters at the moment of electron attachment, the localization process is unique for each trajectory. Nevertheless, the feature common to all of them is that the excess electron shrinks from ~6 Å to roughly 2.75 Å in less than 1.5 ps. For comparison, the red plot at the left hand side of Fig. 3 shows the distribution of radii of gyration of electrons attached to neutral water clusters at 200 different geometries, while the green plot at the right hand side

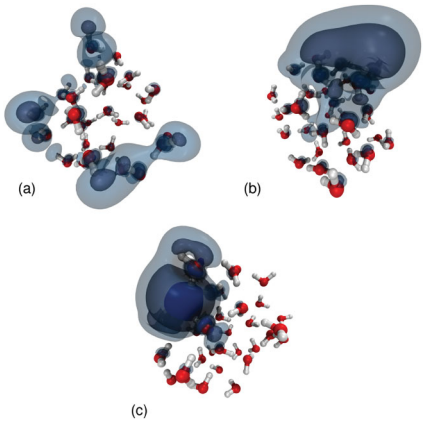

FIG. 1 (color). Snapshots from a representative trajectory at times (a) 0, (b) 950, and (c) 4250 fs after the vertical attachment of the excess electron to a cluster of 32 water molecules at 300 K.

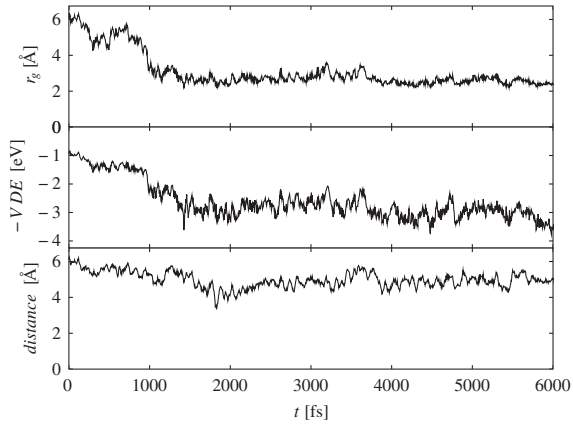

FIG. 2. Time evolution of the radius of gyration (top panel), vertical detachment energy (middle panel), and average distance of the excess electron from the cluster center of mass (bottom panel) for a representative localization trajectory at 300 K.

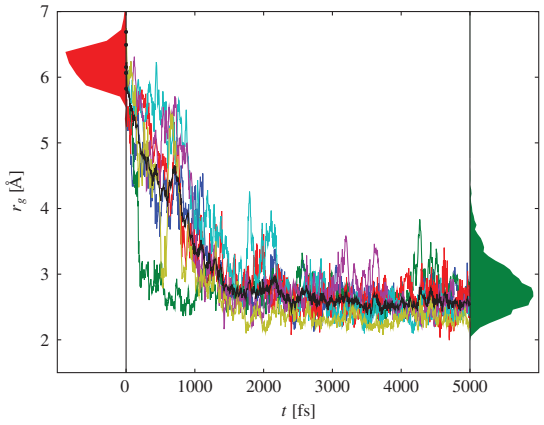

FIG. 3 (color). Time evolution of the radius of gyration of the excess electron in the six localization trajectories at 300 K. Black curve shows the average of these trajectories. Black dots mark the values at $t = 0$ fs. Left, red: distribution of radii of gyration of electrons attached to neutral water clusters. Right, green: distribution of radii of gyration of the solvated electron in equilibrium trajectories.

corresponds to radii of gyration obtained from 40 ps of simulation time of an equilibrium solvated electron. Note that the initial and final distributions of radii of gyration of the localization trajectories match the former and the latter plot, despite the fact that the final distribution is taken from entirely independent simulations.

Let us now move from clusters at ambient temperature to very cold ones. Figure 4 shows the time evolution of the radius of gyration of the excess electron for clusters with mean temperature of 20 or 50 K, compared to those at 300 K. We see that upon moving from warm liquid to cold solid clusters the situation changes dramatically. The initial (subpicosecond) electron localization phase is similar for all temperatures, except that the vertical electron affinity at $t = 0$ is slightly lower in cold clusters. However, at later stages the electron on cold clusters does not localize further, but rather gets trapped in geometries with a radius of gyration between 4 and 5 Å and VDE of 1.3–1.5 eV. Clearly, the initial (partial) reorientation of water molecules is feasible also in the cold glassy clusters, but further stabilization of the electron solvation structure by translational motion of water molecules is hindered at low temperatures. The cold clusters thus get trapped in a metastable situation about half way between the initial geometry and the equilibrated solvated electron. This trapping will persist on much longer time scales than those of the present simulations (up to 15 ps). This is due to the extremely small diffusion rate in amorphous solid water, which is at least 6 orders of magnitude below that in liquid water [35,36]. Therefore, excess electrons attached to cold water clusters are likely to be kinetically trapped in metastable geometries for the micro to millisecond time scales pertinent to the experiment [12,15].

The trapping and nonergodic behavior in cold water clusters is further demonstrated in Fig. 5, which shows the correlation between the radius of gyration of the excess electron and its average distance from the COM of the cluster at different temperatures. Comparison to simulations of an equilibrated solvated electron at 300 K shows again the pronounced difference between localization in warm vs cold clusters. During electron localization at 300 K the system explores the same phase space region as the equilibrated electron (actually an even broader one thanks to the initially strongly delocalized geometries). In cold clusters, however, the excess electron remains localized in a narrow phase space region corresponding to large distances from the cluster center and large to medium values of the radius of gyration. Most notably, at 20 or 50 K the system never visits the region of small radii of gyration, which are characteristic for equilibrium solvated electrons, nor does it leave the outer surface of the cluster. Note that this is not the only possible scenario of formation of cold anionic clusters [15,21], but it is pertinent to cluster experiments used for extrapolations to the liquid bulk [12,20].

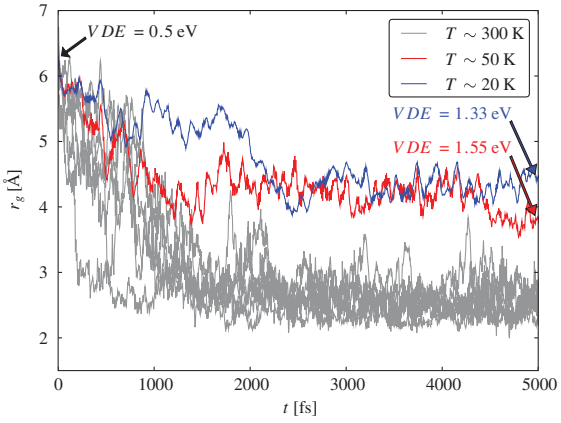

FIG. 4 (color). Time evolution of the radius of gyration of the excess electron in localization trajectories at 20 and 50 K. Arrows with labels show the VDE for both trajectories at the beginning (same geometry for both) and at $t = 5$ ps. Data for 300 K are shown for comparison (gray).

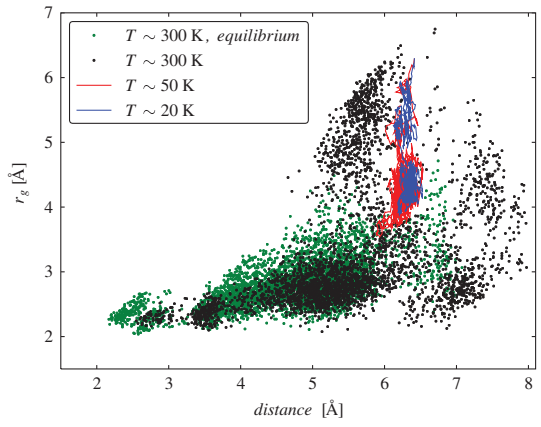

FIG. 5 (color). Correlation between the average distance of the electron from the cluster center of mass and the radius of gyration of the electron. Green: data from equilibrium trajectories at 300 K. Black: data from the first 3 ps of the six localization trajectories at 300 K. Red, blue: data from localization trajectories at 20 and 50 K.

Our simulations shed new light on attempts to extrapolate electron binding energies of different isomers from cold water clusters to the liquid bulk [12,20]. Different experimental conditions lead to effective temperatures of the clusters between 10 and 150 K, where they are solid or at most partially melted [37]. The present simulations of clusters at 20–50 K are most relevant for experiments performed in the lower temperature range, where isomers with weakly bound electrons exist. Experiments show that in such cold clusters several isomers of the excess electron with distinct binding energies can be found [12]. Our simulations support previous suggestions [12,15,19] that most of these isomers are metastable structures kinetically trapped in the glassy clusters. The most stable isomer probably represents an exception, being close to a relaxed structure. This is indicated by the fact that its VDE extrapolates reasonably to the bulk value [15,20,38]. Still, these clusters are about 200 K colder than the liquid bulk and, moreover, at these temperatures, all the less stable isomers are kinetically trapped structures. The present calculations show that in liquid clusters at ambient conditions, which are, however, not readily accessible to experiment due to evaporative cooling, no such distinct isomers exist. The electron, initially attached to a neutral system at 300 K, always relaxes within 1.5 ps into its equilibrated state. Only for this situation, extrapolation of the properties of the excess electron with increasing cluster size to the aqueous bulk is fully justified.

We thank Barbara Kirchner, Joost VandeVondele, Steve Bradforth, Bernd Winter, Katrin Siefermann, and Bernd Abel for fruitful discussions. Support from the Czech Science Foundation (Grant 203/08/0114) and from the Czech Ministry of Education (Grant LC 512) is gratefully acknowledged. O. M. thanks the IMPRS for support.

*pavel.jungwirth@uochb.cas.cz

[1] B. C. Garrett *et al.*, Chem. Rev. **105**, 355 (2005).
[2] P. A. Pieniazek, J. VandeVondele, P. Jungwirth, A. I. Krylov, and S. E. Bradforth, J. Phys. Chem. A **112**, 6159 (2008).
[3] J. Simons, Acc. Chem. Res. **39**, 772 (2006).
[4] P. Kambhampati, D. H. Son, T. W. Kee, and P. F. Barbara, J. Phys. Chem. A **106**, 2374 (2002).
[5] V. H. Vilchiz, J. A. Kloepfer, A. C. Germaine, V. A. Lenchenkov, and S. E. Bradforth, J. Phys. Chem. A **105**, 1711 (2001).
[6] E. Hart and M. Anbar, *The Hydrated Electron* (Wiley-Interscience, New York, 1970).
[7] G. V. Buxton, C. L. Greenstock, W. P. Helman, and A. B. Ross, J. Phys. Chem. Ref. Data **17**, 513 (1988).
[8] R. A. Crowell and D. M. Bartels, J. Phys. Chem. **100**, 17713 (1996).
[9] O. Marsalek, T. Frigato, J. VandeVondele, S. E. Bradforth, B. Schmidt, C. Schütte, and P. Jungwirth, J. Phys. Chem. B **114**, 915 (2010).
[10] C. G. Elles, A. E. Jailaubekov, R. A. Crowell, and S. E. Bradforth, J. Chem. Phys. **125**, 044515 (2006).
[11] J. V. Coe, G. H. Lee, J. G. Eaton, S. T. Arnold, H. W. Sarkas, K. H. Bowen, C. Ludewigt, H. Haberland, and D. R. Worsnop, J. Chem. Phys. **92**, 3980 (1990).
[12] J. R. R. Verlet, A. E. Bragg, A. Kammrath, O. Cheshnovsky, and D. M. Neumark, Science **307**, 93 (2005).
[13] G. B. Griffin, R. M. Young, O. T. Ehrler, and D. M. Neumark, J. Chem. Phys. **131**, 194302 (2009).
[14] N. I. Hammer, J.-W. Shin, J. M. Headrick, E. G. Diken, J. R. Roscioli, G. H. Weddle, and M. A. Johnson, Science **306**, 675 (2004).
[15] L. Ma, K. Majer, F. Chirot, and B. von Issendorff, J. Chem. Phys. **131**, 144303 (2009).
[16] R. N. Barnett, U. Landman, C. L. Cleveland, and J. Jortner, J. Chem. Phys. **88**, 4429 (1988).
[17] J. Xu and K. D. Jordan, J. Phys. Chem. A **114**, 1364 (2010).
[18] H. M. Lee, S. B. Suh, P. Tarakeshwar, and K. S. Kim, J. Chem. Phys. **122**, 044309 (2005).
[19] L. Turi, W.-S. Sheu, and P. J. Rossky, Science **309**, 914 (2005).
[20] K. R. Siefermann, Y. Liu, E. Lugovoy, O. Link, M. Faubel, U. Buck, B. Winter and B. Abel, Nature Chem. **2**, 274 (2010).
[21] A. Madarasz, P. J. Rossky, and L. Turi, J. Phys. Chem. A **114**, 2331 (2010).
[22] V. Buch, B. Sigurd, J. Paul Devlin, U. Buck, and J. K. Kazimirski, Int. Rev. Phys. Chem. **23**, 375 (2004).
[23] A. D. Becke, Phys. Rev. A **38**, 3098 (1988).
[24] C. Lee, W. Yang, and R. G. Parr, Phys. Rev. B **37**, 785 (1988).
[25] S. Grimme, J. Comput. Chem. **27**, 1787 (2006).
[26] S. Goedecker, M. Teter, and J. Hutter, Phys. Rev. B **54**, 1703 (1996).
[27] G. Lippert, J. Hutter, and M. Parrinello, Mol. Phys. **92**, 477 (1997).
[28] J. VandeVondele and M. Sprik, Phys. Chem. Chem. Phys. **7**, 1363 (2005).
[29] J. VandeVondele and J. Hutter, J. Chem. Phys. **127**, 114105 (2007).
[30] L. Genovese, T. Deutsch, and S. Goedecker, J. Chem. Phys. **127**, 054704 (2007).
[31] T. Frigato, J. VandeVondele, B. Schmidt, C. Schütte, and P. Jungwirth, J. Phys. Chem. A **112**, 6125 (2008).
[32] R. N. Barnett, U. Landman, and A. Nitzan, J. Chem. Phys. **91**, 5567 (1989).
[33] I. A. Shkrob, J. Phys. Chem. A **111**, 5223 (2007).
[34] J. VandeVondele, M. Krack, F. Mohamed, M. Parrinello, T. Chassaing, and J. Hutter, Comput. Phys. Commun. **167**, 103 (2005).
[35] K.-H. Jung, S.-C. Park, J.-H. Kim, and H. Kang, J. Chem. Phys. **121**, 2758 (2004).
[36] R. S. Smith, Z. Dohnalek, G. A. Kimmel, K. P. Stevenson, and B. D. Kay, Chem. Phys. **258**, 291 (2000).
[37] C. Hock, M. Schmidt, R. Kuhnen, C. Bartels, L. Ma, H. Haberland, and B. v. Issendorff, Phys. Rev. Lett. **103**, 073401 (2009).
[38] A. T. Shreve, T. A. Yen, and D. M. Neumark, Chem. Phys. Lett. **493**, 216 (2010).